CHALMERS
FINITE ELEMENT CENTER

PREPRINT 2000-06

Discontinuous Galerkin Methods for Incompressible and Nearly Incompressible Elasticity by Nitsche's Method

Peter Hansbo and Mats G. Larson

Chalmers Finite Element Center
CHALMERS UNIVERSITY OF TECHNOLOGY
Göteborg Sweden 2001

CHALMERS FINITE ELEMENT CENTER

Preprint 2000-06

Discontinuous Galerkin Methods for Incompressible and Nearly Incompressible Elasticity by Nitsche's Method

Peter Hansbo and Mats G. Larson

CHALMERS

Chalmers Finite Element Center
Chalmers University of Technology
SE–412 96 Göteborg Sweden
Göteborg, January 2001

Discontinuous Galerkin Methods for Incompressible and Nearly Incompressible Elasticity by Nitsche's Method
Peter Hansbo and Mats G. Larson
NO 2000-06
ISSN 1404–4382

Chalmers Finite Element Center
Chalmers University of Technology
SE–412 96 Göteborg
Sweden
Telephone: +46 (0)31 772 1000
Fax: +46 (0)31 772 3595
www.phi.chalmers.se

Printed in Sweden
Chalmers University of Technology
Göteborg, Sweden 2001

DISCONTINUOUS GALERKIN METHODS FOR INCOMPRESSIBLE AND NEARLY INCOMPRESSIBLE ELASTICITY BY NITSCHE'S METHOD

PETER HANSBO AND MATS G. LARSON

ABSTRACT. We propose and analyze a discontinuous finite element method for nearly incompressible linear elasticity, on triangular or tetrahedral meshes. We show optimal error estimates that are uniform with respect to Poisson's ratio. The method is thus locking free. We also introduce an equivalent mixed formulation, allowing for completely incompressible elasticity problems. Numerical results are presented.

1. INTRODUCTION

Nearly incompressible elasticity displays severe locking problems when low order standard nodal-based displacement methods are used. In engineering practice, this problem is usually circumvented by use of special numerical integration schemes with under-integration of the divergence terms. It is well known that this is equivalent with certain mixed finite element methods using lower order approximation of the Lagrange multiplier (which corresponds to the divergence), see Malkus and Hughes [12]. Another approach is to use non-conforming finite element methods, for instance a linear approximation with relaxed continuity requirements, cf. Brenner and Sung [6] and Kouhia and Stenberg [11].

In this paper, we instead propose the use of a classical discontinuous Galerkin method of Nitsche [13], further developed and analyzed, in the case of scalar elliptic and parabolic problems, by Baker [2], Wheeler [16], and Arnold [1] in the late seventies. Similar approaches have recently been explored, again for scalar elliptic problems, by Freund [10], Oden, Babuška, and Baumann [14], and, for domain decomposition purposes, by Becker and Hansbo [4].

The Nitsche approach allows for independent approximations on different elements, and the continuity of the solution across interelement boundaries, as well as the boundary conditions, are enforced weakly, in such a way that the resulting discrete scheme is consistent with the original partial differential equation. Furthermore, the direct approximation of the elasticity operator

---

Date: January 29, 2001.

Key words and phrases. Incompressible elasticity, discontinuous Galerkin, Nitsche's method, a priori error estimates.

Peter Hansbo, Department of Solid Mechanics, Chalmers University of Technology, S–412 96 Göteborg, Sweden, *email*:hansbo@solid.chalmers.se

Mats G. Larson, Department of Mathematics, Chalmers University of Technology, S–412 96 Göteborg, Sweden, *email*:mgl@math.chalmers.se

Supported by the Swedish Foundation for Strategic Research and the Swedish Council for Engineering Research.

results in a symmetric positve definite system of equations with the same condition number as a standard finite element method of $O(h^{-2})$, where h is the meshsize.

We analyze the Nitsche method and show that the extra flexibility obtained by using discontinuous approximation together with properly chosen stabilization terms result in a locking free method with optimal order convergence.

Next, we formulate a mixed version of the Nitsche method, which is useful in the incompressible limit (Stokes' problem). We establish the stability of the method and state optimal a priori error estimates. Furthermore, for certain parameter values the mixed scheme is equivalent to the single field scheme, and thus we obtain a new proof of our earlier a priori error estimates.

The paper is organized as follows: in Section 2 we state the equations of linear elasticity and discuss the problem of locking and possible remedies; in Sections 3 and 4, we formulate and anlyze the single field and mixed Nitsche method, respectively; we also present illustrative numerical examples. Finally, in Section 5, we give some concluding remarks.

2. The equations of linear elasticity and locking

We consider the equations of linear elasticity in two dimensions: Find the displacement $\boldsymbol{u} = [u_i]_{i=1}^2$ and the symmetric stress tensor $\boldsymbol{\sigma} = [\sigma_{ij}]_{i,j=1}^2$ such that

$$
\begin{aligned}
\boldsymbol{\sigma} &= \lambda\, \nabla\cdot \boldsymbol{u}\boldsymbol{I} + 2\mu\boldsymbol{\varepsilon}(\boldsymbol{u}) && \text{in } \Omega,\\
-\nabla\cdot\boldsymbol{\sigma} &= \boldsymbol{f} && \text{in } \Omega,\\
\boldsymbol{u} &= \boldsymbol{g} && \text{on } \partial\Omega_{\mathrm{D}},\\
\boldsymbol{\sigma}\cdot\boldsymbol{n} &= \boldsymbol{h} && \text{on } \partial\Omega_{\mathrm{N}}.
\end{aligned}
\tag{2.1}
$$

Here Ω is a closed subset of $\mathbb{R}^2$, λ and μ are positive constants called the Lamé constants, satisfying $0 < \mu_1 < \mu < \mu_2$ and $0 < \lambda < \infty$, and $\boldsymbol{\varepsilon}(\boldsymbol{u}) = [\varepsilon_{ij}(\boldsymbol{u})]_{i,j=1}^2$ is the strain tensor with components

$$
\varepsilon_{ij}(\boldsymbol{u}) = \frac{1}{2}\left(\frac{\partial u_i}{\partial x_j} + \frac{\partial u_j}{\partial x_i}\right).
$$

Furthermore, $\nabla\cdot\boldsymbol{\sigma} = \left[\sum_{j=1}^2 \partial\sigma_{ij}/\partial x_j\right]_{i=1}^2$, $\boldsymbol{I} = [\delta_{ij}]_{i,j=1}^2$ with $\delta_{ij} = 1$ if $i = j$ and $\delta_{ij} = 0$ if $i \neq j$, $\boldsymbol{f}$ and $\boldsymbol{h}$ are given loads, $\boldsymbol{g}$ is a given boundary displacement, and $\boldsymbol{n}$ is the outward unit normal to $\partial\Omega$. In terms of the modulus of elasticity, E, and Poisson's ratio, ν, we have, in the case of plane strain, that $\lambda = E\nu/((1+\nu)(1-2\nu))$ and $\mu = E/(2(1+\nu))$.

Incompressible behavior is obtained as the parameter $\lambda \to \infty$, i.e., as $\nu \to 1/2$. In such cases the performance of standard conforming methods will deteriorate, a phenomenon known as *locking*. To alleviate locking, several approaches exist; some well-known examples are:

- Mixed finite element approximations with additional unknowns representing the divergence of the displacement. The problem with this approach is that as the material tends to the incompressible limit, the selection of the discrete spaces cannot be selected independently of each other. This problem is discussed, e.g., in the textbook by Brezzi and Fortin [7].
- Under-integration of the divergence term. This idea is related to the mixed approach, cf. [12], and will not work unless the under-integration is sufficiently severe.

- Non-conforming methods with reduced continuity requirements on the displacements. This approach requires that the resulting scheme fulfills a discrete version of Korn's inequality to ensure coercivity of the discrete operator. For an example of such a method, see [11].
- Stabilized finite element methods, e.g., of Galerkin/least-squares type. This approach is similar to a mesh dependent relaxation of the incompressibility condition, as suggested by Brezzi and Pitkäranta [9].

In this paper we propose a new possibility: a consistent relaxation of the continuity requirements using a version of a method originally proposed by Nitsche [13]. Using this approach, we do not need to use under-integration, we do not need to introduce additional variables, and we do not need to prove a discrete Korn's inequality. The main, and serious, drawback of our approach lies in the increased number of degrees of unknowns as compared with a continuous method of the same order of convergence. We emphasize that this work should be viewed as a first step towards investigating the possibilities inherent in the framework of discontinuous approximations for higher-order differential operators.

3. A discontinuous Galerkin method

3.1. **Formulation of the discontinuous Galerkin method.** Consider a subdivision of Ω into a geometrically conforming simplicial finite element partitioning $\mathcal{T}^h = \{T\}$ of Ω. Let

$$P^k(T) = \{\boldsymbol{v}\text{: each component of } \boldsymbol{v} \text{ is a polynomial of degree} \leq k \text{ on } T\},$$

$$\boldsymbol{W}^h = \{\boldsymbol{v} \in [L^2(\Omega)]^2 : \ \boldsymbol{v}|_T \in P^k(T)\ \forall T \in \mathcal{T}^h\},$$

let ∂T_{int} denote the sides of the element T neighboring to other elements, ∂T_{N} the sides neighboring to $\partial\Omega_{\text{N}}$, and ∂T_{D} the sides neighboring to $\partial\Omega_{\text{D}}$. Further, let $\boldsymbol{n}_T$ denote the outward pointing normal to ∂T, and, for $\boldsymbol{x} \in \partial T$, let $[\boldsymbol{U}] = \boldsymbol{U}^+ - \boldsymbol{U}^-$ and $\langle \boldsymbol{U} \rangle = (\boldsymbol{U}^+ + \boldsymbol{U}^-)/2$, where $\boldsymbol{U}^\pm = \lim_{\epsilon\downarrow 0} \boldsymbol{U}(\boldsymbol{x} \mp \epsilon\, \boldsymbol{n}_T)$.

We seek a function $\boldsymbol{U} \in \boldsymbol{W}^h$ such that

$$a_h(\boldsymbol{U}, \boldsymbol{v}) = L_h(\boldsymbol{v}) \quad \text{for all } \boldsymbol{v} \in \boldsymbol{W}^h. \tag{3.1}$$

The bilinear form $a_h(\cdot,\cdot)$ and linear functional $L_h(\cdot)$ are sums of element contributions $a_h(\boldsymbol{U}, \boldsymbol{v}) = \sum_T a_T(\boldsymbol{U}, \boldsymbol{v})$ and $L_h(\boldsymbol{v}) = \sum_T L_T(\boldsymbol{v})$ defined by

$$\begin{aligned} a_T(\boldsymbol{U}, \boldsymbol{v}) \ = \ & \int_T \boldsymbol{\sigma}(\boldsymbol{U}) : \boldsymbol{\varepsilon}(\boldsymbol{v})\, dx \\ & -\frac{1}{2}\int_{\partial T_{\text{int}}} \left(\langle \boldsymbol{\sigma}(\boldsymbol{U}) \cdot \boldsymbol{n}_T \rangle \cdot [\boldsymbol{v}] + \langle \boldsymbol{\sigma}(\boldsymbol{v}) \cdot \boldsymbol{n}_T \rangle \cdot [\boldsymbol{U}] \right)\, ds \\ & +\frac{\mu}{2}\int_{\partial T_{\text{int}}} \frac{\gamma_\mu}{h} [\boldsymbol{U}] \cdot [\boldsymbol{v}]\ ds + \frac{\lambda}{2}\int_{\partial T_{\text{int}}} \frac{\gamma_\lambda}{h} [\boldsymbol{U} \cdot \boldsymbol{n}_T]\ [\boldsymbol{v} \cdot \boldsymbol{n}_T]\ ds \\ & -\int_{\partial T_{\text{D}}} \left(\boldsymbol{\sigma}(\boldsymbol{U}) \cdot \boldsymbol{n}_T \cdot \boldsymbol{v} + \boldsymbol{\sigma}(\boldsymbol{v}) \cdot \boldsymbol{n}_T \cdot \boldsymbol{U} \right)\, ds \\ & +\mu \int_{\partial T_{\text{D}}} \frac{\gamma_\mu}{h} \boldsymbol{U} \cdot \boldsymbol{v}\, ds + \lambda \int_{\partial T_{\text{D}}} \frac{\gamma_\lambda}{h} \boldsymbol{U} \cdot \boldsymbol{n}_T\, \boldsymbol{v} \cdot \boldsymbol{n}_T\, ds, \end{aligned} \tag{3.2}$$

where we have used the notation $\boldsymbol{\sigma} : \boldsymbol{\varepsilon} = \sum_i \sum_j \sigma_{ij}\varepsilon_{ij}$, and the linear functional is given by

$$L_T(\boldsymbol{v}) = \int_T \boldsymbol{f}\cdot\boldsymbol{v}\,dx + \int_{\partial T_{\rm N}} \boldsymbol{h}\cdot\boldsymbol{v}\,ds - \int_{\partial T_{\rm D}} \boldsymbol{\sigma}(\boldsymbol{v})\cdot\boldsymbol{n}_T\cdot\boldsymbol{g}\,ds + \mu\int_{\partial T_{\rm D}} \frac{\gamma_\mu}{h}\boldsymbol{g}\cdot\boldsymbol{v}\,ds + \lambda\int_{\partial T_{\rm D}} \frac{\gamma_\lambda}{h}\boldsymbol{g}\cdot\boldsymbol{n}_T\,\boldsymbol{v}\cdot\boldsymbol{n}_T\,ds. \tag{3.3}$$

Here, on each edge E, the mesh parameter h is defined by

$$h|_E = \begin{cases} 2\left(\dfrac{\text{length}(E)}{\text{area}(T^+)} + \dfrac{\text{length}(E)}{\text{area}(T^-)}\right)^{-1} & \text{for } E \subset \partial T^+ \cap \partial T^-, \\ \text{area}(T)/\text{length}(E) & \text{for } E \subset \partial T \cap \partial\Omega. \end{cases} \tag{3.4}$$

Remark. This definition of the mesh parameter h on each edge makes it possible to calculate, explicitly, suitable values for the parameters γ_μ and γ_λ in (3.2) that are independent of the size and shape of the triangles. However, assuming a quasi-uniform mesh, one may use some other equivalent choice of mesh parameter, for instance, the length of the edge.

By use of Green's formula, we readily establish the following proposition.

Proposition 3.1. *The method* (3.1) *is consistent in the sense that*

$$a_h(\boldsymbol{u} - \boldsymbol{U}, \boldsymbol{v}) = 0$$

for all $\boldsymbol{v} \in \boldsymbol{W}^h$ *and for* $\boldsymbol{u}$ *sufficiently regular.*

3.2. **A priori error estimates.** For the purpose of error analysis, we introduce the following mesh dependent energy norm

$$|||\boldsymbol{v}|||^2 = \sum_{T\in\mathcal{T}^h} |||\boldsymbol{v}|||_T^2, \tag{3.5}$$

where the element contributions $|||\boldsymbol{v}|||_T$ are defined by

$$|||\boldsymbol{v}|||_T^2 = 2\mu\Big(\|\boldsymbol{\varepsilon}(\boldsymbol{v})\|^2_{L^2(T)} + \frac{1}{2}\left\|h^{-1/2}[\boldsymbol{v}]\right\|^2_{L^2(\partial T_{\rm int})} + \left\|h^{-1/2}\boldsymbol{v}\right\|^2_{L^2(\partial T_{\rm D})}\Big) + \lambda\Big(\|\nabla\cdot\boldsymbol{v}\|^2_{L^2(T)} + \frac{1}{2}\left\|h^{-1/2}[\boldsymbol{v}\cdot\boldsymbol{n}]\right\|^2_{L^2(\partial T_{\rm int})} + \left\|h^{-1/2}\boldsymbol{v}\cdot\boldsymbol{n}\right\|^2_{L^2(\partial T_{\rm D})}\Big), \tag{3.6}$$

where, for tensors,

$$\|\boldsymbol{\varepsilon}(\boldsymbol{v})\|^2_{L^2(T)} = \int_T \boldsymbol{\varepsilon}(\boldsymbol{v}) : \boldsymbol{\varepsilon}(\boldsymbol{v})\,dx.$$

The mesh dependent norm $|||\cdot|||$ can be used to bound the broken $H^1(\Omega)$ norm on $\boldsymbol{W}^h$, which we show in the following proposition.

Proposition 3.2. *There is a constant* C, *independent of* h, μ, *and* λ *such that*

$$\sum_{T\in\mathcal{T}^h} \|\boldsymbol{v}\|^2_{H^1(T)} \le C|||\boldsymbol{v}|||^2 \quad \textit{for all } \boldsymbol{v} \in \boldsymbol{W}^h. \tag{3.7}$$

Proof. Assume that the right-hand side of (3.7) is zero. It then follows that

$$\|\boldsymbol{\varepsilon}(\boldsymbol{v})\|_{L^2(T)} = 0,$$

and therefore $\boldsymbol{v}|_T \in RM(T)$, where

$$RM(T) = \{\boldsymbol{v} \in P^k(T) : \ \boldsymbol{v}(\boldsymbol{x}) = \boldsymbol{a}_T + b_T\,(-x_2, x_1), \ \boldsymbol{a}_T \in \mathbb{R}^2, \ b_T \in \mathbb{R}\} \tag{3.8}$$

is the space of linearized rigid body motions on T. Next, using that

$$\|[\boldsymbol{v}]\|_{L^2(\partial T)} = 0,$$

we conclude that there are constants $\boldsymbol{a}$ and b such that $\boldsymbol{a} = \boldsymbol{a}_T$ and $b = b_T$, for all triangles T. Furthermore, from $\|\boldsymbol{v}\|_{L^2(\partial\Omega_{\mathrm{D}})} = 0$ it follows that $\boldsymbol{a} = \boldsymbol{0}$ and $b = 0$. Thus, if the right-hand side of (3.7) is zero, so is the left-hand side, since $0 < \mu_1 < \mu$ for some positive constant μ_1. Finally, finite dimensionality, together with scaling, yields the result. □

In order to show that the method (3.1) is stable, we shall show that $a_h(\cdot,\cdot)$ is coercive with respect to the norm $|||\cdot|||$, given that γ_μ and γ_λ are chosen large enough. In order to do so, we need the following inverse inequalities.

Lemma 3.1. *For $\boldsymbol{v} \in P_k(T)$ there are constants C_μ and C_λ, independent of the diameter h, such that*

$$\left\|h^{1/2}\boldsymbol{\varepsilon}(\boldsymbol{v})\cdot\boldsymbol{n}\right\|^2_{L^2(\partial T)} \le C_\mu \|\boldsymbol{\varepsilon}(\boldsymbol{v})\|^2_{L^2(T)}, \tag{3.9}$$

$$\left\|h^{1/2}\nabla\cdot\boldsymbol{v}\right\|^2_{L^2(\partial T)} \le C_\lambda \|\nabla\cdot\boldsymbol{v}\|^2_{L^2(T)}, \tag{3.10}$$

where on each edge $E \subset \partial T$ the meshsize h is defined by $h = area(T)/length(E)$. If, in addition, T is a straight-edged triangle, C_μ and C_λ are also independent of the minimal angle of the triangle T.

Proof. To prove (3.9) we note that if the right hand side is zero, we have $\boldsymbol{v} \in RM(T)$, where $RM(T)$ is defined in (3.8) and thus the left hand side is also zero. For (3.10) we note that since $\boldsymbol{v}$ is a polynomial, $\|\nabla\cdot\boldsymbol{v}\|_{L^2(T)} = 0$ implies $\nabla\cdot\boldsymbol{v} = 0$ pointwise, and thus $\|h^{1/2}\nabla\cdot\boldsymbol{v}\|_{L^2(\partial T)} = 0$. Both estimates, (3.9) and (3.10), now follow from finite dimensionality and scaling from a unit reference element.

Furthermore, if T has straight edges, then T is the image of a reference triangle under an affine mapping and therefore the quotient

$$C_{\mu,E} = \sup_{\boldsymbol{v}\in P^k(T)} \frac{\mathrm{length}(E)^{-1}\displaystyle\int_E \boldsymbol{\varepsilon}(\boldsymbol{v})\cdot\boldsymbol{n}\cdot\boldsymbol{\varepsilon}(\boldsymbol{v})\cdot\boldsymbol{n}}{\mathrm{area}(T)^{-1}\displaystyle\int_T \boldsymbol{\varepsilon}(\boldsymbol{v}):\boldsymbol{\varepsilon}(\boldsymbol{v})}, \tag{3.11}$$

where E is an edge of the triangle T, is independent of the size and shape of the triangle T. This is seen by mapping to the reference element and using the fact that the determinant of the Jacobian is constant. Now simply define $C_\mu = 3C_{\mu,E}$, since there are three edges. □

Remark. Here we shall calculate upper bounds of the constants C_μ and C_λ. From the proof of Lemma 3.1 we have $C_\mu = 3C_{\mu,E}$. Further $C_{\mu,E}$ is the maximum eigenvalue of the eigenvalue problem

$$A\hat{\boldsymbol{v}} = \lambda B\hat{\boldsymbol{v}}, \tag{3.12}$$

where $\hat{\boldsymbol{v}}$ denotes the coordinates of $\boldsymbol{v}$ in a basis $\{\boldsymbol{\varphi}_j\}$ for $P^k(T)$,

$$A_{ij} = \int_E \boldsymbol{n}\cdot\boldsymbol{\varepsilon}(\boldsymbol{\varphi}_i)\cdot\boldsymbol{n}\cdot\boldsymbol{\varepsilon}(\boldsymbol{\varphi}_j)\,ds,$$

and

$$B_{ij} = \int_T \boldsymbol{\varepsilon}(\boldsymbol{\varphi}_i) : \boldsymbol{\varepsilon}(\boldsymbol{\varphi}_j)\,dx.$$

We can treat C_λ in a similar manner. Solving these eigenvalue problems numerically and multiplying the maximum eigenvalue by three, give the following values for C_μ and C_λ. Note that the constant increases with the order of the polynomials p.

	p=1	p=2	p=3	p=4
C_μ	1.6875	5.0625	10.1249	16.2948
C_λ	1.5000	4.5000	9.0000	15.0000

We are now ready to show our coercivity result.

Proposition 3.3. *If $\gamma_{\mu;\lambda} \geq 2m + C_{\mu;\lambda}/4(1-m)$, for $0 < m < 1$, then the following estimate holds*

$$m\,|||\boldsymbol{v}|||^2 \leq a_h(\boldsymbol{v},\boldsymbol{v}) \quad \textit{for all } \boldsymbol{v} \in \boldsymbol{W}^h, \tag{3.13}$$

independent of h. The constants C_μ and C_λ are defined in Lemma 3.1.

Proof. Setting $\boldsymbol{U} = \boldsymbol{v}$ in the definition of the the bilinear form (3.2) we obtain

$$\begin{aligned} a_h(\boldsymbol{v},\boldsymbol{v}) &= \sum_{T\in\mathcal{T}^h} 2\mu\Big(\|\boldsymbol{\varepsilon}(\boldsymbol{v})\|^2_{L^2(T)} - \frac{1}{2}\int_{\partial T}\langle \boldsymbol{n}_T\cdot\boldsymbol{\varepsilon}(\boldsymbol{v})\rangle\cdot[\boldsymbol{v}]\,ds \\ &\qquad + \frac{\gamma_\mu}{2}\left\|h^{-1/2}[\boldsymbol{v}]\right\|^2_{L^2(\partial T)}\Big) \\ &\quad + \sum_{T\in\mathcal{T}^h} \lambda\Big(\|\nabla\cdot\boldsymbol{v}\|_{L^2(T)} - \frac{1}{2}\int_{\partial T}\langle\nabla\cdot\boldsymbol{v}\rangle\,[\boldsymbol{n}_T\cdot\boldsymbol{v}]\,ds \\ &\qquad + \frac{\gamma_\lambda}{2}\left\|h^{-1/2}[\boldsymbol{n}_T\cdot\boldsymbol{v}]\right\|^2_{L^2(\partial T)}\Big) \\ &= I + II, \end{aligned} \tag{3.14}$$

with the obvious notation and modification where $\partial T \cap \partial\Omega \neq \emptyset$. To show the coercivity we need to bound the potentially negative terms by the positive terms. We begin with an estimate of the second term in I. Using the Cauchy–Schwarz inequality, followed by the inverse inequality (3.9) in Lemma 3.1, we have

$$\begin{aligned}\sum_{T\in\mathcal{T}^h}\int_{\partial T}\langle \boldsymbol{n}_T\cdot\boldsymbol{\varepsilon}(\boldsymbol{v})\rangle\cdot[\boldsymbol{v}]\,ds \\ &\leq \sum_{T\in\mathcal{T}^h}\left\|h^{1/2}\langle \boldsymbol{n}_T\cdot\boldsymbol{\varepsilon}(\boldsymbol{v})\rangle\right\|_{L^2(\partial T)}\left\|h^{-1/2}[\boldsymbol{v}]\right\|_{L^2(\partial T)} \\ &\leq \sum_{T\in\mathcal{T}^h}\left\|h^{1/2}\boldsymbol{n}_T\cdot\boldsymbol{\varepsilon}(\boldsymbol{v})\right\|_{L^2(\partial T)}\left\|h^{-1/2}[\boldsymbol{v}]\right\|_{L^2(\partial T)} \\ &\leq \sum_{T\in\mathcal{T}^h} C_\mu\left\|h^{1/2}\boldsymbol{\varepsilon}(\boldsymbol{v})\right\|_{L^2(T)}\left\|h^{-1/2}[\boldsymbol{v}]\right\|_{L^2(\partial T)} \\ &\leq \sum_{T\in\mathcal{T}^h}\epsilon_\mu C_\mu^2\left\|h^{1/2}\boldsymbol{\varepsilon}(\boldsymbol{v})\right\|_{L^2(T)}^2+\frac{1}{4\epsilon_\mu}\left\|h^{-1/2}[\boldsymbol{v}]\right\|_{L^2(\partial T)}^2,\end{aligned}$$

where we finally used the inequality $ab \leq a^2/(2\epsilon)+\epsilon b^2/2$, for $a,b,\epsilon\in\mathbb{R}, \epsilon>0$. Choosing $\epsilon_\mu=(1-m)/C_\mu^2$ and $\gamma_\mu \geq 2m+1/4\epsilon_\mu = 2m + C_\mu^2/4(1-m)$ we get

$$\begin{aligned} I &\geq \sum_{T\in\mathcal{T}^h} 2\mu\Bigg(\left(1-\epsilon_\mu C_\mu^2\right)\|\boldsymbol{\varepsilon}(\boldsymbol{v})\|_{L^2(T)}^2 \\ &\qquad +\left(\frac{\gamma_\mu}{2}-\frac{1}{8\epsilon_\mu}\right)\left\|h^{-1/2}\,[\boldsymbol{v}]\right\|_{L^2(\partial T)}^2\Bigg) \\ &\geq m2\mu\left(\|\boldsymbol{\varepsilon}(\boldsymbol{v})\|_{L^2(T)}^2+\left\|h^{-1/2}[\boldsymbol{v}]\right\|_{L^2(\partial T)}^2\right) \qquad (3.15)\end{aligned}$$

Exactly the same technique may be used to prove that II, choosing $\epsilon_\lambda=(1-m)/C_\lambda^2$ and $\gamma_\mu \geq 2m + C_\lambda^2/4(1-m)$ we get

$$II \geq m\lambda\left(\|\nabla\cdot\boldsymbol{v}\|_{L^2(T)}^2+\left\|h^{-1/2}[\boldsymbol{n}_T\cdot\boldsymbol{v}]\right\|_{L^2(\partial T)}^2\right). \qquad (3.16)$$

Together (3.14), (3.15), and (3.16), yields the desired estimate. □

For the proof of our main a priori error estimate we need to introduce the interpolation operator of Brezzi, Douglas, and Marini, see [8] and the book by Brezzi and Fortin [7]. We summarize its properties in the following lemma.

Lemma 3.2. *If the mesh consists of triangles in two dimensions or tetrahedra in three dimensions there is an interpolation operator $\boldsymbol{\pi}_{BDM} : H^1(\Omega) \to \boldsymbol{W}^h$ with the following properties:*

1. $[\boldsymbol{n}\cdot\boldsymbol{\pi}_{BDM}\boldsymbol{u}]=0$,
2. $\|\boldsymbol{u}-\boldsymbol{\pi}_{BDM}\boldsymbol{u}\|_{H^m(T)} \leq Ch_T^{l-m}\|\boldsymbol{u}\|_{H^l(T)}$, *with* $m=0,1,2$, *and* $m\leq l\leq k+1$,
3. $\|\nabla\cdot(\boldsymbol{u}-\boldsymbol{\pi}_{BDM}\boldsymbol{u})\|_{H^m(T)} \leq Ch_T^{l-m}\|\nabla\cdot\boldsymbol{u}\|_{H^l(T)}$, *with* $m=0,1$, *and* $m\leq l\leq k$,
4. $\int_T v(\nabla\cdot\boldsymbol{u}-\nabla\cdot\boldsymbol{\pi}_{BDM}\boldsymbol{u})dx=0$, *for all* $v\in P^{k-1}(T)$,

5. $\int_E v(\boldsymbol{n}\cdot\boldsymbol{u} - \boldsymbol{n}\cdot\boldsymbol{\pi}_{BDM}\boldsymbol{u})ds = 0$, *for all* $v \in P^k(E)$, *where* E *is an edge or face on* ∂T, *for all* $\boldsymbol{u} \in H^{k+1}(T)$.

Proof. See Propositions III.3.6, III.3.7, and III.3.8 in Brezzi and Fortin [7]. □

We are now ready to formulate our main result.

Theorem 3.1. *With* $\boldsymbol{U}$ *the solution of* (3.1) *and* $\boldsymbol{u}$ *the solution of* (2.1), *we have that*

$$|||\boldsymbol{U}-\boldsymbol{u}||| \leq Ch^k\Big((2\mu)^{1/2}\|\boldsymbol{u}\|_{H^{k+1}(\Omega)} + \lambda^{1/2}\|\nabla\cdot\boldsymbol{u}\|_{H^k(\Omega)}\Big).$$

Here, $C = C_1 + C_2/m$, *where* C_1 *and* C_2 *are independent of* h, μ, *and* λ.

Proof. Using the notation $\boldsymbol{v} = \boldsymbol{\pi}_{BDM}\boldsymbol{u}$ and $\boldsymbol{\eta} = \boldsymbol{u} - \boldsymbol{\pi}_{BDM}\boldsymbol{u}$, we have

$$|||\boldsymbol{U}-\boldsymbol{u}||| \leq |||\boldsymbol{U}-\boldsymbol{v}||| + |||\boldsymbol{\eta}|||. \tag{3.17}$$

From coercivity, Proposition 3.3, and concistency, Proposition 3.1, it follows that

$$\begin{aligned} m|||\boldsymbol{U}-\boldsymbol{v}|||^2 &\leq a_h(\boldsymbol{U}-\boldsymbol{v},\boldsymbol{U}-\boldsymbol{v}) \\ &= a_h(\boldsymbol{\eta},\boldsymbol{U}-\boldsymbol{v}). \end{aligned} \tag{3.18}$$

Next, using the definition (3.2) of $a_h(\cdot,\cdot)$ and the inverse estimates in Lemma 3.1 we get

$$\begin{aligned} a_h(\boldsymbol{\eta},\boldsymbol{U}-\boldsymbol{v}) \;\leq\; & C|||\boldsymbol{U}-\boldsymbol{v}|||\Big(|||\boldsymbol{\eta}||| + \sum_{T\in\mathcal{T}^h}(2\mu)^{1/2}\left\|h^{1/2}\boldsymbol{n}\cdot\boldsymbol{\varepsilon}(\boldsymbol{\eta})\right\|_{L^2(\partial T)} \\ & + \sum_{T\in\mathcal{T}^h}\lambda^{1/2}\left\|h^{1/2}\nabla\cdot\boldsymbol{\eta}\right\|_{L^2(\partial T)}\Big). \end{aligned} \tag{3.19}$$

Combining (3.17), (3.18), and (3.19) we get the estimate

$$\begin{aligned} |||\boldsymbol{u}-\boldsymbol{U}||| \;\leq\; & \Big(1+\frac{C}{m}\Big)|||\boldsymbol{\eta}||| + \sum_{T\in\mathcal{T}^h}(2\mu)^{1/2}\left\|h^{1/2}\boldsymbol{n}\cdot\boldsymbol{\varepsilon}(\boldsymbol{\eta})\right\|_{L^2(\partial T)} \\ & + \sum_{T\in\mathcal{T}^h}\lambda^{1/2}\left\|h^{1/2}\nabla\cdot\boldsymbol{\eta}\right\|_{L^2(\partial T)}. \end{aligned} \tag{3.20}$$

We now proceed with estimates of the three different terms on the right hand side of (3.20). To deal with the boundary terms we need the following trace inequality

$$\|\boldsymbol{w}\|^2_{L^2(\partial T)} \leq C\|\boldsymbol{w}\|_{L^2(T)}\Big(h_T^{-1}\|\boldsymbol{w}\|_{L^2(T)} + \|\boldsymbol{w}\|_{H^1(T)}\Big) \quad \boldsymbol{w}\in H^1(T), \tag{3.21}$$

where C is independent of the diameter of the triangle h_T. This inequality is obtained by mapping T onto the unit size reference element T_{ref}, invoking the trace inequality

$$\|\boldsymbol{w}\|^2_{L^2(\partial T_{\text{ref}})} \leq C\|\boldsymbol{w}\|_{L^2(T_{\text{ref}})}\|\boldsymbol{w}\|_{H^1(T_{\text{ref}})} \quad \boldsymbol{w}\in H^1(T_{\text{ref}}), \tag{3.22}$$

see [5], and finally transforming back to T.

We begin with an estimate of the first term on the right hand side of (3.20). Starting from the definition of the energy norm (3.5) and using the crucial fact that $[\boldsymbol{n}\cdot\boldsymbol{\eta}] = 0$, cf.

(1) in Lemma 3.2, and the triangle inequality to split the remaining jump contributions, we obtain

$$
\begin{aligned}
|||\boldsymbol{\eta}|||^2 &\leq \sum_{T\in\mathcal{T}^h} 2\mu\Big(\|\boldsymbol{\varepsilon}(\boldsymbol{\eta})\|^2_{L^2(T)} + \frac{1}{2}\left\|h^{-1/2}\boldsymbol{\eta}\right\|^2_{L^2(\partial T)}\Big) + \lambda\,\|\nabla\cdot\boldsymbol{\eta}\|^2_{L^2(T)} \\
&\leq \sum_{T\in\mathcal{T}^h} C2\mu\Big(h_T^{-2}\,\|\boldsymbol{\eta}\|^2_{L^2(T)} + h_T^{-1}\,\|\boldsymbol{\eta}\|_{L^2(T)}\,\|\boldsymbol{\eta}\|_{H^1(T)} + \|\boldsymbol{\eta}\|^2_{H^1(T)}\Big) \\
&\qquad + \lambda\,\|\nabla\cdot\boldsymbol{\eta}\|^2_{L^2(T)} \\
&\leq Ch_T^{2k}\Big(2\mu\,\|\boldsymbol{u}\|^2_{H^{k+1}(\Omega)} + \lambda\,\|\nabla\cdot\boldsymbol{u}\|^2_{H^k(\Omega)}\Big), \qquad (3.23)
\end{aligned}
$$

where we used the trace inequality (3.21), followed by interpolation error estimates (2) and (3) in Lemma 3.2 to estimate the right hand side. Note that the constant C is independent of h, μ, and λ.

Next we estimate the second term in (3.20). Using the trace inequality (3.21), followed by the interpolation error estimate (2) in Lemma 3.2, we obtain

$$
\begin{aligned}
\left\|h^{1/2}\boldsymbol{n}\cdot\boldsymbol{\varepsilon}(\boldsymbol{\eta})\right\|^2_{L^2(\partial T)} &\leq Ch_T\,\|\boldsymbol{\varepsilon}(\boldsymbol{\eta})\|_{L^2(T)}\Big(h_T^{-1}\,\|\boldsymbol{\varepsilon}(\boldsymbol{\eta})\|_{L^2(T)} + \|\boldsymbol{\varepsilon}(\boldsymbol{\eta})\|_{H^1(T)}\Big) \\
&\leq C\Big(\|\boldsymbol{\eta}\|^2_{H^1(T)} + h_T\,\|\boldsymbol{\eta}\|_{H^1(T)}\,\|\boldsymbol{\eta}\|_{H^2(T)}\Big) \\
&\leq Ch_T^{2k}\,\|\boldsymbol{u}\|^2_{H^{k+1}(T)}\,. \qquad (3.24)
\end{aligned}
$$

Finally, in the same way as for the second term, but this time invoking (3) in Lemma 3.2, we get, for the last term in (3.20),

$$
\begin{aligned}
\left\|h^{1/2}\nabla\cdot\boldsymbol{\eta}\right\|^2_{L^2(\partial T)} &\leq Ch_T\,\|\nabla\cdot\boldsymbol{\eta}\|_{L^2(T)}\Big(h_T^{-1}\,\|\nabla\cdot\boldsymbol{\eta}\|_{L^2(T)} + \|\nabla\cdot\boldsymbol{\eta}\|_{H^1(T)}\Big) \\
&\leq C\Big(\|\nabla\cdot\boldsymbol{\eta}\|^2_{L^2(T)} + h_T\,\|\nabla\cdot\boldsymbol{\eta}\|_{L^2(T)}\,\|\nabla\cdot\boldsymbol{\eta}\|_{H^1(T)}\Big) \\
&\leq Ch_T^{2k}\,\|\nabla\cdot\boldsymbol{u}\|^2_{H^k(T)}\,. \qquad (3.25)
\end{aligned}
$$

Collecting (3.20) and the estimates (3.23), (3.24), and (3.25), the theorem follows. The constant is clearly of the form in the theorem and independent of h, μ, and λ, since we have made the depencies of theses parameters explicit in each step of the proof. □

Combining the error estimate in Theorem 3.1 with the elliptic regularity estimate

$$
\begin{aligned}
&\|\boldsymbol{u}\|_{H^{k+1}(\Omega)} + \frac{1}{1-2\nu}\,\|\nabla\cdot\boldsymbol{u}\|_{H^k(\Omega)} \qquad (3.26) \\
&\qquad \leq C\Big(\|\boldsymbol{f}\|_{H^{k-1}(\Omega)} + \|\boldsymbol{g}\|_{H^{k+1/2}(\partial\Omega_D)} + \|\boldsymbol{h}\|_{H^{k-1/2}(\partial\Omega_N)}\Big),
\end{aligned}
$$

(valid uniformly in ν, cf. Vogelius [15]) we obtain the following estimate in terms of data, which shows that the method does not lock as $\lambda \to \infty$.

Corollary 3.1. *There is a constant C, independent of h, μ, and λ such that the following estimate holds*

$$\|\|\boldsymbol{u} - \boldsymbol{U}\|\| \leq Ch^k \Big(\|\boldsymbol{f}\|_{H^{k-1}(\Omega)} + \|\boldsymbol{g}\|_{H^{k+1/2}(\partial\Omega_D)} + \|\boldsymbol{h}\|_{H^{k-1/2}(\partial\Omega_N)} \Big). \tag{3.27}$$

3.3. **Numerical example.** We consider the "driven cavity flow" problem, common in fluid flow applications. The domain is $\Omega = (0,1) \times (0,1)$, and the boundary conditions are given by: On $\partial\Omega_1 = \{x_2 = 1 \text{ and } 0 < x_1 < 1\}$ we set $\boldsymbol{u} = (1,0)$ and on $\partial\Omega \setminus \partial\Omega_1$ we set $\boldsymbol{u} = (0,0)$. In Fig. 1 we show computational results using a standard conforming finite element method (left column) and the proposed method (right column) for modulus of elasticity $E = 1$ and Poisson's ratio

$$\nu = \{0.49, 0.499, 0.4999\}.$$

The continuous, conforming, method displays visible locking problem for $\nu > 0.49$, whereas the discontinuous method is completely robust with respect to locking. In Fig. 2 we show the computational mesh; the displacement fields shown in Fig. 1 are obtained by evaluation in the midpoint of each element. Finally, in Fig. 3, we show the $L_2(\Omega)-$norm of the difference between the continuous and discontinuous solutions as a function of Poisson's ratio.

4. A mixed discontinuous Galerkin method

In this section, we shall formulate and analyze a mixed discontinuous Galerkin method. Such a method is of interest in its own right for approximating mixed problems corresponding to the case of an incompressible material or the Stokes problem modeling incompressible fluid flow.

Furthermore, from the analysis of the mixed method we obtain a new error estimate, which complements Theorem 3.1, for the single field method. In particular, it follows that the single field method does not lock in the incompressible limit. For an alternative discontinuous Galerkin method for the Stokes problem, using continuous pressure and discontinuous piecewise solenoidal velocity, see Baker, Jureidini, and Karakashian [3].

4.1. **Formulation of the mixed discontinuous Galerkin method.** To formulate a mixed version of (3.1), we make the identification

$$P|_T = (-\lambda \nabla \cdot \boldsymbol{U})|_T,$$

so that $P \in Q^h$, where

$$Q^h = \{q \in L^2(\Omega) : \ q|_T \in P^{k-1}(T) \ \forall T \in \mathcal{T}^h\}, \tag{4.1}$$

and consider the mixed problem of finding $(\boldsymbol{U}, P) \in \boldsymbol{W}^h \times Q^h$ such that

$$\tilde{a}_h(\boldsymbol{U}, \boldsymbol{v}) + b_h(\boldsymbol{U}, q) + b_h(\boldsymbol{v}, P) - c_h(P, q) = L_h(\boldsymbol{v}, q) \tag{4.2}$$

for all $(\boldsymbol{v}, q) \in \boldsymbol{W}^h \times Q^h$, where again the forms are sums of element contributions defined by

$$
\begin{aligned}
\tilde{a}_T(\boldsymbol{U},\boldsymbol{v}) = & \int_T 2\mu\,\boldsymbol{\varepsilon}(\boldsymbol{U}) : \boldsymbol{\varepsilon}(\boldsymbol{v})\,dx \\
& - \frac{1}{2}\int_{\partial T_{\text{int}}} \left(\langle 2\mu\,\boldsymbol{\varepsilon}(\boldsymbol{U})\cdot\boldsymbol{n}_T\rangle\cdot[\boldsymbol{v}] + \langle 2\mu\,\boldsymbol{\varepsilon}(\boldsymbol{v})\cdot\boldsymbol{n}_T\rangle\cdot[\boldsymbol{U}]\right)\,ds \\
& + \frac{\mu}{2}\int_{\partial T_{\text{int}}} \frac{\gamma_\mu}{h}\,[\boldsymbol{U}]\cdot[\boldsymbol{v}]\,ds + \frac{\lambda}{2}\int_{\partial T_{\text{int}}} \frac{\gamma_\lambda}{h}\,[\boldsymbol{U}\cdot\boldsymbol{n}_T]\,[\boldsymbol{v}\cdot\boldsymbol{n}_T]\,ds \\
& - \int_{\partial T_{\text{D}}} \left(2\mu\,\boldsymbol{\varepsilon}(\boldsymbol{U})\cdot\boldsymbol{n}_T\cdot\boldsymbol{v} + 2\mu\,\boldsymbol{\varepsilon}(\boldsymbol{v})\cdot\boldsymbol{n}_T\cdot\boldsymbol{U}\right)\,ds \\
& + \mu\int_{\partial T_{\text{D}}} \frac{\gamma_\mu}{h}\boldsymbol{U}\cdot\boldsymbol{v}\,ds + \lambda\int_{\partial T_{\text{D}}} \frac{\gamma_\lambda}{h}\boldsymbol{U}\cdot\boldsymbol{n}_T\,\boldsymbol{v}\cdot\boldsymbol{n}_T\,ds,
\end{aligned} \tag{4.3}
$$

$$
b_T(\boldsymbol{v},q) = \int_T -q\,\nabla\cdot\boldsymbol{v}\,dx + \frac{1}{2}\int_{\partial T_{\text{int}}} \langle q\rangle\,[\boldsymbol{v}\cdot\boldsymbol{n}_T]\,ds, + \int_{\partial T_{\text{D}}} q\,\boldsymbol{v}\cdot\boldsymbol{n}_T\,ds, \tag{4.4}
$$

$$
c_T(P,q) = \int_T \frac{1}{\lambda}P\,q\,dx, \tag{4.5}
$$

and the linear functional by

$$
\begin{aligned}
L_T(\boldsymbol{v},q) = & \int_T \boldsymbol{f}\cdot\boldsymbol{v}\,dx + \int_{\partial T_{\text{N}}} \boldsymbol{h}\cdot\boldsymbol{v}\,ds - \int_{\partial T_{\text{D}}} 2\mu\boldsymbol{\varepsilon}(\boldsymbol{v})\cdot\boldsymbol{n}_T\cdot\boldsymbol{g}\,ds \\
& + \int_{\partial T_{\text{D}}} q\,\boldsymbol{n}_T\cdot\boldsymbol{g}\,ds + \mu\int_{\partial T_{\text{D}}} \frac{\gamma_\mu}{h}\boldsymbol{g}\cdot\boldsymbol{v}\,ds + \lambda\int_{\partial T_{\text{D}}} \frac{\gamma_\lambda}{h}\boldsymbol{g}\cdot\boldsymbol{n}_T\,\boldsymbol{v}\cdot\boldsymbol{n}_T\,ds.
\end{aligned} \tag{4.6}
$$

Note that the incompressible limit $\lambda \to \infty$ corresponds to $c_T(\cdot,\cdot) = 0$.

4.2. **A priori error estimates.** For the analysis of the mixed method we introduce the norms

$$
\|\boldsymbol{v}\|_{\boldsymbol{W}^h}^2 = \sum_{T\in\mathcal{T}^h} 2\mu\left(\|\boldsymbol{\varepsilon}(\boldsymbol{v})\|_{L^2(T)}^2 + \frac{1}{2}\left\|h^{-1/2}[\boldsymbol{v}]\right\|_{\partial T_{\text{int}}}^2 + \left\|h^{-1/2}\boldsymbol{v}\right\|_{\partial T_{\text{D}}}^2\right), \tag{4.7}
$$

$$
\|q\|_{Q^h}^2 = \sum_{T\in\mathcal{T}^h} \|q\|_{L^2(T)}^2 . \tag{4.8}
$$

As is well known, see Brezzi and Fortin [7], the existence of a solution to (4.2) satisfying optimal error estimates is a direct consequence of the stability conditions in the following proposition.

Proposition 4.1. *If $\gamma_\mu \geq \alpha + C_\mu/4(1-\alpha)$ and $\gamma_\lambda \geq 0$, then there exists a constant α, with $0 < \alpha < 1$, such that*

$$
\alpha\,\|\boldsymbol{v}\|_{\boldsymbol{W}^h}^2 \leq \tilde{a}_h(\boldsymbol{v},\boldsymbol{v}) \quad \textit{for all } \boldsymbol{v}\in\boldsymbol{W}^h. \tag{4.9}
$$

Furthermore, there is a constant $\beta > 0$ such that

$$
\beta \leq \inf_{q\in Q^h}\sup_{\boldsymbol{v}\in\boldsymbol{W}^h} \frac{b_h(\boldsymbol{v},q)}{\|\boldsymbol{v}\|_{\boldsymbol{W}^h}\,\|q\|_{Q^h}}. \tag{4.10}
$$

Proof. The first statement (4.9) follows in the same way as in the proof of Proposition 3.3.

To prove the inf-sup condition (4.10) we first show that the inf-sup condition (4.10) holds with $\boldsymbol{W}$ replaced by $H^1(\Omega)$ and then we use properties of the interpolation operator $\boldsymbol{\pi}_{\mathrm{BDM}}$ to prove (4.10).

Let $q \in Q^h$ be given. Defining $\boldsymbol{v}_q = \nabla\varphi$, where φ satisfies

$$-\Delta\varphi = q \quad \text{in } \Omega, \qquad \boldsymbol{n}\cdot\nabla\varphi = 0 \quad \text{on } \partial\Omega,$$

gives $-\nabla\cdot\boldsymbol{v}_q = q$ in Ω, $\boldsymbol{n}\cdot\boldsymbol{v}_q = 0$ on $\partial\Omega$, and $[\boldsymbol{n}_T\cdot\boldsymbol{v}_q] = 0$ on each interior edge. Starting from the definition (4.4) of $b_h(\cdot,\cdot)$ and using the properties of $\boldsymbol{v}$ we obtain the identity

$$b_h(\boldsymbol{v}_q, q) = \|q\|^2_{Q^h}\,. \tag{4.11}$$

Furthermore, using elliptic regularity we have

$$\|\boldsymbol{v}_q\|_{H^1(\Omega)} \le \|\nabla\varphi\|_{H^1(\Omega)} \le C\,\|q\|_{L^2(\Omega)}\,. \tag{4.12}$$

Combining (4.11) and (4.12) it follows that

$$\sup_{\boldsymbol{v}\in H^1(\Omega)} \frac{b_h(\boldsymbol{v},q)}{\|\boldsymbol{v}\|_{H^1(\Omega)}} \ge \frac{b_h(\boldsymbol{v}_q,q)}{\|\boldsymbol{v}_q\|_{H^1(\Omega)}} \ge \beta'\,\|q\|_{Q^h}\,, \tag{4.13}$$

with $\beta' = 1/C > 0$, independent of $q \in Q^h$.

We shall now replace $\boldsymbol{v}_q$ with $\boldsymbol{\pi}_{\mathrm{BDM}}\boldsymbol{v}_q$ and show that the inf-sup condition (4.10) holds. First, we conclude that

$$b_h(\boldsymbol{v},q) = b_h(\pi_{\mathrm{BDM}}\boldsymbol{v},q) \quad \text{for } \boldsymbol{v}\in H^1(\Omega), q\in Q^h, \tag{4.14}$$

using the definition (4.4) of $b_h(\cdot,\cdot)$, properties (4) and (5) in Lemma 3.2, and the fact that $q \in Q^h$ is a piecewise polynomial of degree $k-1$. Next we note that first using the trace inequality (3.21) to bound the contributions from the boundaries of the triangles to $\|\boldsymbol{v}\|_{\boldsymbol{W}^h}$, and then using the interpolation error estimate (2), with $m = l = 1$, in Lemma 3.2 we get

$$\|\boldsymbol{v} - \pi_{\mathrm{BDM}}\boldsymbol{v}\|_{\boldsymbol{W}^h} \le C\,\|\boldsymbol{v}\|_{H^1(\Omega)}\,.$$

Using the triangle inequality we conclude that the following stability estimate holds

$$\|\pi_{\mathrm{BDM}}\boldsymbol{v}\|_{\boldsymbol{W}^h} \le C\,\|\boldsymbol{v}\|_{H^1(\Omega)} \quad \text{for } \boldsymbol{v}\in H^1(\Omega), \tag{4.15}$$

since $\|\boldsymbol{v}\|_{\boldsymbol{W}^h} \le C\,\|\boldsymbol{v}\|_{H^1(\Omega)}$, using the trace inequality (3.22) to estimate the contribution from the Dirichlet boundary.

Using (4.14) and (4.15), and finally (4.13) we obtain

$$\begin{aligned}
\sup_{\boldsymbol{v}\in\boldsymbol{W}^h} \frac{b_h(\boldsymbol{v},q)}{\|\boldsymbol{v}\|_{\boldsymbol{W}^h}} &\ge \frac{b_h(\boldsymbol{\pi}_{\mathrm{BDM}}\boldsymbol{v}_q,q)}{\|\boldsymbol{\pi}_{\mathrm{BDM}}\boldsymbol{v}_q\|_{\boldsymbol{W}^h}} \\
&\ge \frac{b_h(\boldsymbol{v}_q,q)}{C\,\|\boldsymbol{v}_q\|_{H^1(\Omega)}} \\
&\ge \frac{\beta'}{C}\,\|q\|_{Q^h}\,,
\end{aligned}$$

independent of the choice of $q \in Q^h$, and thus the desired result follows with $\beta = \beta'/C > 0$. □

Remark. Note that to establish the coercivity with respect to $\boldsymbol{W}^h$, does not require $\gamma_\lambda > 0$, and thus we may choose $\gamma_\lambda = 0$ when implementing the mixed method. In fact, this is the natural choice. However, for equivalence with (3.1) we need to keep this term in the formulation. The equivalence is necessary for the analysis of the mixed method to hold also for the single field method.

We are thus ready to state a standard a priori error estimate for the mixed method. Here, we are only interested in the limiting case of $\lambda \to \infty$; the identification $P|_T = (-\lambda \nabla \cdot \boldsymbol{U})|_T$, together with uniqueness of the solution to the mixed problem, shows that the solution to the mixed problem is in fact identical to that of (3.1) for λ finite.

Theorem 4.1. *Let $\boldsymbol{U}$ be the solution of (4.2) and $\boldsymbol{u}$ the solution of (2.1) and assume that the assumptions in Proposition 4.1 hold. Then, in the limit $\lambda \to \infty$, we have the error estimate*

$$\|\boldsymbol{U} - \boldsymbol{u}\|_{\boldsymbol{W}^h} + \|P - p\|_{Q^h} \le Ch^k\Big(\|\boldsymbol{u}\|_{H^{k+1}(\Omega)} + \|p\|_{H^k(\Omega)}\Big).$$

Here the constant C depends on the constants α and β defined in Proposition 4.1, but is independent of h, μ, and λ.

Proof. This follows from the stability properties of Proposition 4.1 and the approximation properties of the polynomial spaces used; for details, see Brezzi and Fortin [7]. □

4.3. **Numerical example.** We show the effect of varying the stability parameter γ_μ. The domain and boundary conditions are the same as in Section 3.3.

In Fig. 4, we show the typical checkerboarding pattern in the pressure variable, resulting from an injudicious choice of $\gamma_\mu = 6000$. Choosing γ_μ this large means enforcing the continuity of the related conforming mixed method, which is not stable. In Fig. 5, we show the corresponding stable solution for $\gamma_\mu = 6$. For ease of presentation, we show the L_2-projection of the discontinuous pressure onto the space of piecewise linear, continuous, functions.

5. Concluding remarks

In this paper, we have proposed a weakly conforming, discontinuous, and piecewise polynomial finite element method for incompressible and nearly incompressible elasticity. Numerical examples support the theoretical results that

(i) the proposed method does not lock in the limit of Poisson's ratio tending to 1/2 (i.e., the error estimates hold uniformly in λ),
(ii) the corresponding mixed method is stable in the sense of Babuška and Brezzi.

Our approach has the disadvantage of introducing many more unknowns than the corresponding continuous finite element method of the same polynomial degree. Nevertheless, we believe that it has some distinct advantages: it is more general than the continuous finite element method, which it contains as a special case, and it enables the use of different polynomial degree of approximation on adjacent elements, as well as the use of non-matching meshes.

References

[1] D. N. Arnold, An interior penalty finite element method with discontinuous elements, SIAM J. Numer. Anal. **19** (1982) 742–760.

[2] G. A. Baker, Finite element methods for elliptic equations using nonconforming elements, Math. Comp. **31** (1977) 45–59.

[3] G. A. Baker, W. N. Jureidini, and O. A. Karakashian, Piecewise solenoidal vector fields and the Stokes problem, SIAM J. Numer. Anal. **27** (1990) 1466–1485.

[4] R. Becker and P. Hansbo, A finite element method for domain decomposition with non-matching grids, INRIA Research Report No. 3613 (1999).

[5] S.C. Brenner and L.R. Scott, The Mathematical Theory of Finite Element Methods, Springer Verlag, 1994.

[6] S. C. Brenner and L. Sung, Linear finite element methods for planar linear elasticity, Math. Comp. **59** (1992) 321–338

[7] F. Brezzi and M. Fortin, Mixed and Hybrid Finite Element Methods, Springer Verlag, 1991.

[8] F. Brezzi, J. Douglas, and D. Marini, Two families of mixed finite elemeents for second order elliptic problems, Numer. Math. 47, 217-235, 1985.

[9] F. Brezzi and J. Pitkäranta, On the stabilization of finite element approximations of the Stokes equations, in: *Efficient Solution of Elliptic Systems*, W. Hackbusch (ed.), (Vieweg, 1984)

[10] J. T. Freund, The discontinuous Galerkin method for a scalar elliptic equation, in: *Computational Mechanics: New Trends and Applications,* S. Idehlson, E. Oñate, and E. Dvorkin (eds.), (CIMNE, 1998)

[11] R. Kouhia and R. Stenberg, A linear nonconforming finite element method for nearly incompressible elasticity and Stokes flow, Comput. Methods Appl. Mech. Engrg. **124** (1995) 195–212.

[12] D. S. Malkus and T. J. R. Hughes, Mixed finite element methods—reduced and selective integration techniques: a unification of concepts, Comput. Methods Appl. Mech. Engrg. **15** (1978) 63–81.

[13] J. Nitsche, Über ein Variationsprinzip zur Lösung von Dirichlet-Problemen bei Verwendung von Teilräumen, die keinen Randbedingungen unterworfen sind, Abh. Math. Univ. Hamburg **36** (1970) 9–15.

[14] J. T. Oden, I. Babuška, and C. E. Baumann, A discontinuous *hp* finite element method for diffusion problems, J. Comput. Phys. **146** (1998) 491-519

[15] M. Vogelius, An analysis of the p–version of the finite element method for nearly incompressible materials: Uniformly valid, optimal error estimates, Numer. Math. **41** (1983) 39–53.

[16] M. F. Wheeler, An elliptic collocation-finite element method with interior penalties, SIAM J. Numer. Anal. **15** (1978) 152–161.

[17] V. Thomée, *Galerkin Finite Element Methods for Parabolic Problems*, (Springer, 1997)

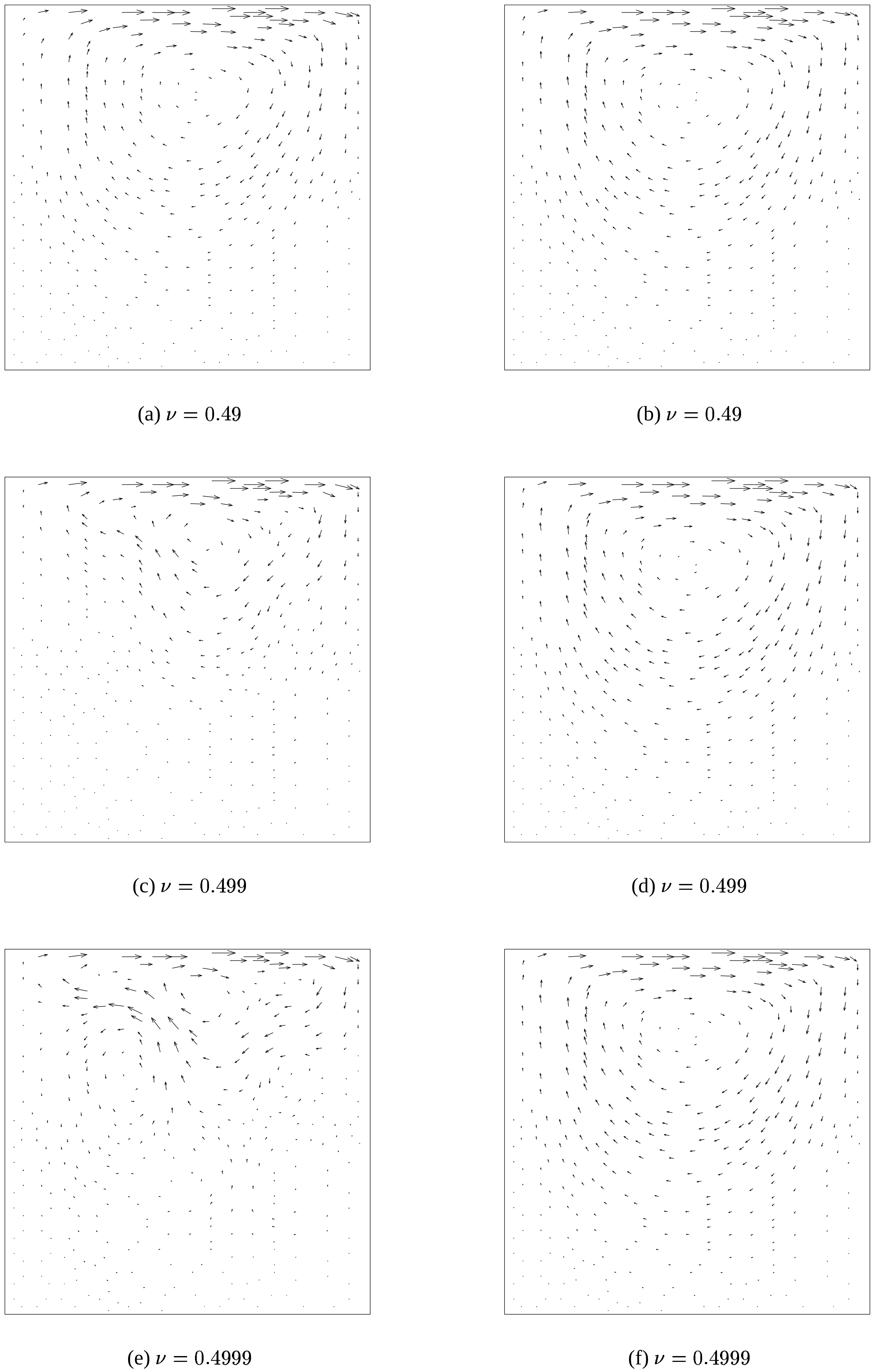

FIGURE 1. Locking. Continuous (left) and discontinuous (right) finite element method for $\nu \to 1/2$ (increasing from top to bottom).

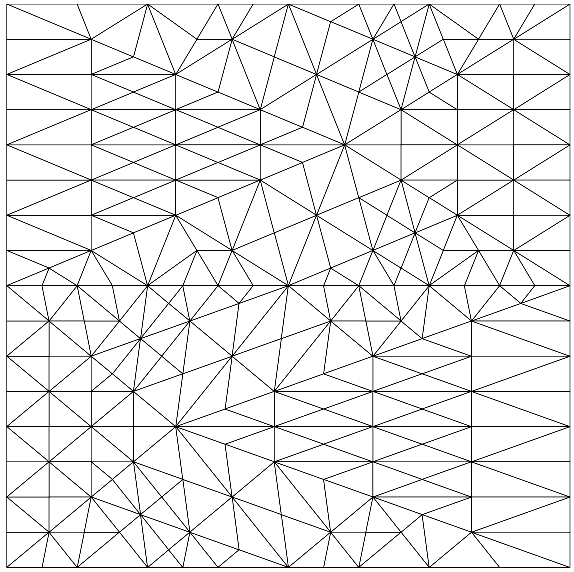

FIGURE 2. Computational mesh.

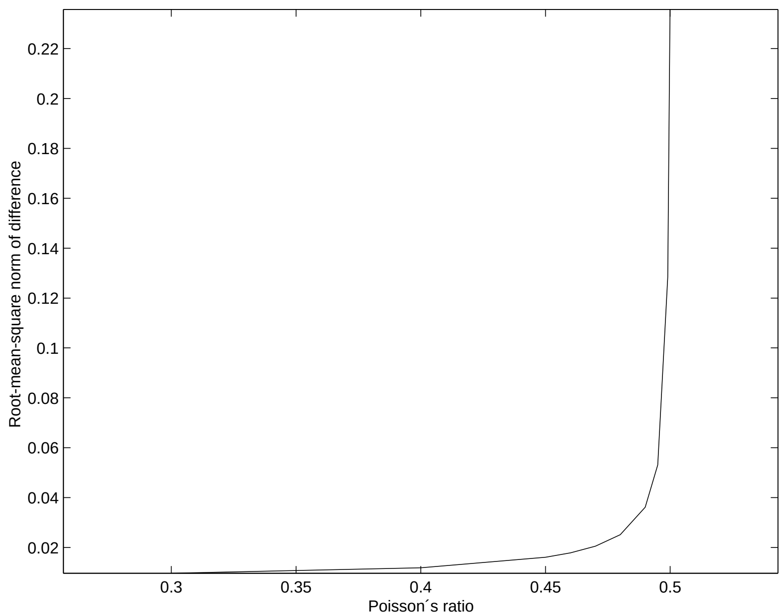

FIGURE 3. L_2-norm of the difference between the continuous and discontinuous solutions as a function of ν.

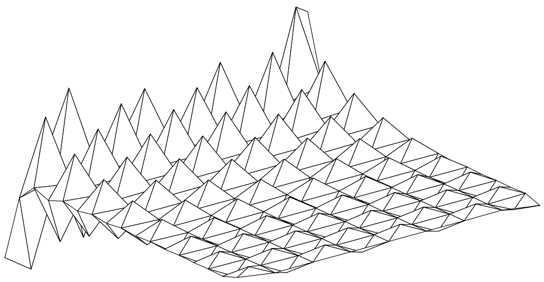

(a) Pressure

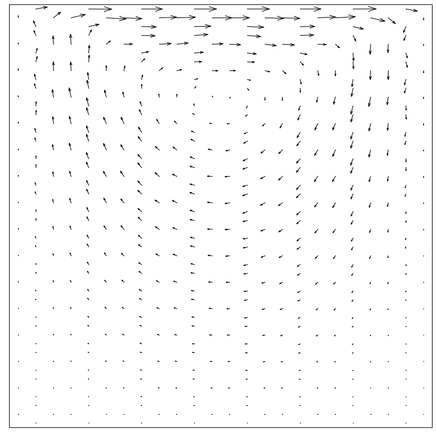

(b) Velocity

FIGURE 4. Pressure checkerboarding for $\gamma_\mu >> 1$.

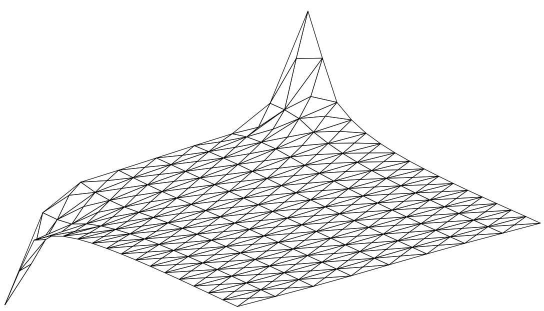

(a) Pressure

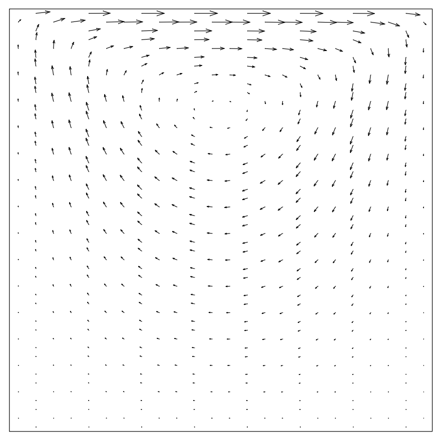

(b) Velocity

FIGURE 5. Stable solution for moderate-sized γ_μ.

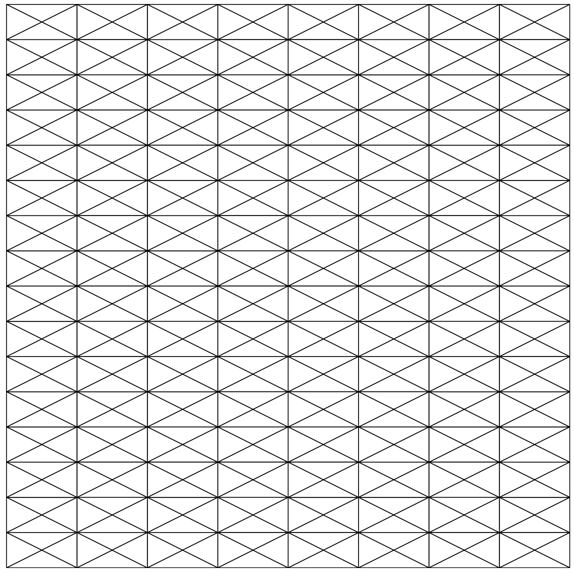

FIGURE 6. Computational mesh.

CHALMERS FINITE ELEMENT CENTER PREPRINTS

2000–01 *Adaptive Finite Element Methods for the Unsteady Maxwell's Equations*
Johan Hoffman

2000–02 *A Multi-Adaptive ODE-Solver*
Anders Logg

2000–03 *Multi-Adaptive Error Control for ODEs*
Anders Logg

2000–04 *Dynamic Computational Subgrid Modeling* (Licentiate Thesis)
Johan Hoffman

2000–05 *Least-Squares Finite Element Methods for Electromagnetic Applications* (Licentiate Thesis)
Rickard Bergström

2000–06 *Discontinuous Galerkin methods for incompressible and nearly incompressible elasticity by Nitsche's method*
Peter Hansbo and Mats G. Larson

These preprints can be obtained from

`www.phi.chalmers.se/preprints`